NUMERICAL SIMULATION STEADY STATE OPERATION FLOW OF THE FRANCIS-99 TURBINE USING RANS/LES TURBULENCE MODEL

[1,2]Platonov D., [1,2]Minakov A., [1,2]Sentyabov A., [1,2]Gavrilov A.

[1]Siberian Federal University, Krasnoyarsk, Russia

[2]Institute of Thermophysics SB RAS, Novosibirsk, Russia,

Abstract

Abstract. We performed numerical simulation of flow in a laboratory model of a Francis hydroturbine at a three regimes, using two eddy-viscosity- (EVM) and a Reynolds stress (RSM) RANS models (realizable k-ε, k-ω SST, LRR) and detached-eddy-simulations (DES), as well as large-eddy simulations (LES). Comparison of calculation results with the experimental data was carried out. Unlike the linear EVMs, the RSM, DES, and LES reproduced well the mean velocity components, and pressure pulsations in the diffusor draft tube. Despite relatively coarse meshes and insufficient resolution of the near-wall region, LES, DES also reproduced well the well the intrinsic flow unsteadiness and the dominant flow structures and the associated pressure pulsations in the draft tube.

Keywords: Francis turbine, numerical simulation, pressure pulsation, the precession of the vortex rope, turbulence, CFD , LES, RANS and DES models.

1. Introduction

An important task of hydropower plant is the regulation of power in the energy system. During load changing, hydraulic units repeatedly undergo off-design modes of operation. In these modes, the flow remains essentially swirling after passing through the water turbine runner. The instability of swirling flow results in the appearance of intense low-frequency hydrodynamic pulsations, which threaten the safety and reliability of turbine structure.

The improvement of hydraulic machines efficiency and failure tolerance is impossible without studying the physical mechanisms of hydrodynamic processes, among which an important role is played by the transient phenomena associated with the formation of large-scale vortex structures. One of the mechanisms responsible for generating flow pulsations is the precessing vortex rope. It is formed downstream the runner under part-load or over-load conditions when the flow has a large residual swirl after passing through the runner [1–5].

The precession of vortex rope can be a serious danger for hydraulic equipment due to powerful flow pulsations that lead to strong vibrations of turbine structure. It the case of resonance, it can result in the turbine structural failure. Pressure pulsations generated by precessing vortex rope may also affect the cavitation process and enhance cavitation erosion. To

predict the resonance phenomena and find the ways of suppressing instability, one needs the detailed information about the characteristics of pulsation regimes and flow structure. It should be noted that the working approaches must meet the requirement of minimizing energy losses (increasing the efficiency of water turbine). It can be realized only through in-depth understanding of hydrodynamic processes occurring in the flow path of a water turbine.

The precession of vortex rope has been studied for quite a long time. These issues have long been in focus of the experimental research complemented by some simplified analytics, but a full account of the three-dimensional time dynamics has remained to a large extent beyond the reach of even most advanced laser-based measurements and diagnostics techniques. Computer simulations have been seen as a potential tool for capturing the subtleties of the development of instabilities and associated vortical and turbulence structures. Such information can be obtained by direct and large-eddy simulations (DNS, LES) over a range of important scales. However, the accuracy of DNS and LES depends much on the numerical resolution. For complex configurations the Reynolds-averaged Navier-Stokes (RANS) approach, being computationally less demanding, has been considered as a more rational option for industrial purposes. However, because if its empirical contents, the RANS have not been regarded as a trustful research tool, and moreover, their credibility depends much on the choice of the turbulence model to close the time- or ensemble-averaged conservation equations.

Despite the extensive literature (e.g. Doerfler [2], Alligne et al. [6], comprehensive experimental data for hydroturbines are still scarce, apart from mean velocity and second-moment turbulence statistics measured at selected locations in laboratory models of some popular turbine types [7-8]. On the other hand, there are still many open questions regarding the numerical simulation of flows in turbines of realistic configuration and practical relevance. Because of typically very high Re numbers, DNS and even LES, requiring enormous numerical mesh and computer resources, are usually beyond the reach of designers, but also of many researchers, leaving the URANS or hybrid RANS/LES as the only viable routes. Here the first challenge is related to selecting the appropriate RANS model that can reproduce satisfactorily the unsteady flow and the dynamics of at least the dominant large-scale vortex structures subjected to strong swirls, curvature and adverse pressure gradients in complex geometric shapes. The popular linear eddy-viscosity modes (k-ε, k-ω, and their many “improved” variants) lack on sufficient physics and have shown to perform poorly in describing such flows.

We report here the results of simulation of flow in a Francis-99 hydraulic turbine at a three regimes using several RANS models, a DES (detached-eddy simulations) and LES. The models were benchmarked against the experimental data. We discuss the flow patterns and vortical

structure in the turbine draft tube and its impact on flow stability and pressure pulsations, especially at part loads characterized by unsteady helix ropes.

2. Turbulence models

Flows in hydroturbine systems are characterized by several features which pose a challenge to the RANS models. The flows in the guide vanes and the rotating impeller are dominated by the bounding wall – blades and housing, and a strong favourable pressure gradient which for the design operating conditions (no flow separation) can be handled reasonably well with a well-tuned wall-integration (WIN) model that (for the runner) accounts properly for the rotation effects. Accurate predictions of the blade-tip leakage, the follow-up vortical wakes and flow separation on blades at part loads, require more advanced, anisotropy-accounting RANS models. The phenomena in a draft tube are different. Here the flow is governed by a strong swirl and a bluff-body recirculation zone behind the impeller hub, which is usually reinforced by the negative pressure due to the swirl. The 90 degree bend encountered in elbow draft tubes, with a subsequent circular-to-rectangular change of the cross-section further modify the flow especially at part loads creating very complex vortical patterns with additional recirculation and secondary flows. On the other hand, the walls are smooth, and despite a strong elbow curvature, the wall-adjacent azimuthal fluid velocity and turbulence seem to follow reasonably well the common wall scaling so that computations seem manageable by the common wall-integration schemes or, according to some publications, even with using the standard wall-function approach. The apparent success of relatively standard wall treatment could in part be explained by strong radial pressure gradients and by inviscid interactions that diminish the wall effects as well as the role of the employed turbulence model on the dominant vortical structures and the consequent mean flow pattern.

The above brief overview of some major phenomena encountered in hydromachinery illustrate the importance of choosing the proper RANS model, which depends on which phenomena are in the focus of the computations. As stated above, our focus is on the draft tube and, specifically, on the strong and coherent swirling structures, primarily the precessing vortex cores and especially on the undesirable twin-ropes and the associated strong pressure pulsations at part loads. The linear eddy-viscosity (LEVM) turbulence models, widely spread in engineering calculations, are known to describe poorly most features listed above. Nevertheless, we tested some popular models, all validated against a well-resolved dynamic LES, aimed at scrutinizing the ability of various models to capture the above mentioned specific structures and pressure oscillation in the considered draft-tube model.

The computations here reported were performed with the ANSYS-FLUENT code using the built-in two popular eddy-viscosity (k-ω-SST and the realizable k-ε), a Re-stress model (Launder-Reece and Rodi, LRR, with the linear pressure strain and wall-echo terms), and a DES (based on the $k-\omega$ SST Menter's model). In parallel, for reference, LES with the WALE subgrid-scale viscosity model was carried out on finer grids.

The high-Re-number realizable k-ε model and the basic RSM were solved using the standard wall functions. A test with the enhanced wall treatment and the non-equilibrium wall function available in the FLUENT code produced no significant differences in the results. For the $k-\omega$ SST we used the enhanced-wall-treatment ω-equation model (EWT-ω).

A specific issue in the computer simulation of hydraulic turbines is the treatment of the rotating impeller and the rotor-stator interaction. Several approaches can be found in the literature, i.e. dynamic, sliding and moving grid methods, and those based on a moving reference frame. The latter is the most common and the simplest way to model the runner rotation. It assumes that the runner is fixed and the equations are solved in a rotating reference frame. This formulation is often referred to as the "frozen rotor" approach. In this paper, the modelling of the runner rotation was performed in the rotated reference frame for the runner zone. The obtained results are then rotated with the runner rotation speed and as such imposed as the inflow field as the inlet into the draft tube. The earlier test calculations proved that this approach is credible for describing the integral flow characteristics including the dominant flow pulsations [4,5,8-10]. A comparison with the computationally more demanding method using sliding meshes showed that for this type flows with a focus on draft tube dynamics the results are almost the same.

The computations were performed using the finite-volume method on structured grids. The coupling of the velocity and pressure fields for incompressible flow was ensured using the SIMPLE-C procedure. For the URANS models the convective terms in all equation were discretized by a second-order upwind scheme, whereas the second-order central difference scheme was used for LES and DES (in the LES region). The time derivatives were approximated by an implicit second-order scheme. The time step was set from the condition CFL<2, but in the bulk of the draft tube the CFL number was less than 1.0. Some peaks exceeding the value of 2.0 appeared close to the guide-vane and impeller blades. The statistics was gathered for each run during about 10 sec of real time.

3. Computational domain, boundary conditions and grids

The computational domain included all the elements constituting the turbine system (spiral casing, guide vane, impeller and draft tube) see (Fig.1). The 3D geometry of the turbine has been taken on the website workshop Francis (2016). Since the intake channel was not considered in

the calculations, the boundary conditions were set at the inlet to the turbine spiral casing by imposing a total head measured in the experiment and taken from Table 1. As the LES method requires initial time-dependent forcing mimicking turbulence, random velocity fluctuations were imposed at the inlet, generated by the method proposed in [11].

Table 1. Acquired flow parameters and other quantities during steady state measurements.

Parameter	PL	BEP	HL
Guide vane angle (°)	6.72	9.84	12.43
Net head (m)	11.87	11.94	11.88
Discharge ($m^3\ s^{-1}$)	0.13962	0.19959	0.24246
Torque to the generator (Nm)	416.39	616.13	740.54
Friction torque (Nm)	4.40	4.52	3.85
Runner angular speed (rpm)	332.84	332.59	332.59
Casing inlet pressure-abs (kPa)	218.08	215.57	212.38
Draft tube outlet pressure-abs (kPa)	113.17	111.13	109.59
Hydraulic efficiency (%)	90.13	92.39	91.71
Water density ($kg\ m^{-3}$)	999.8	999.8	999.8
Kinematic viscosity ($m^2\ s^{-1}$)	9.57E-7	9.57E-7	9.57E-7
Gravity ($m\ s^{-2}$)	9.82	9.82	9.82

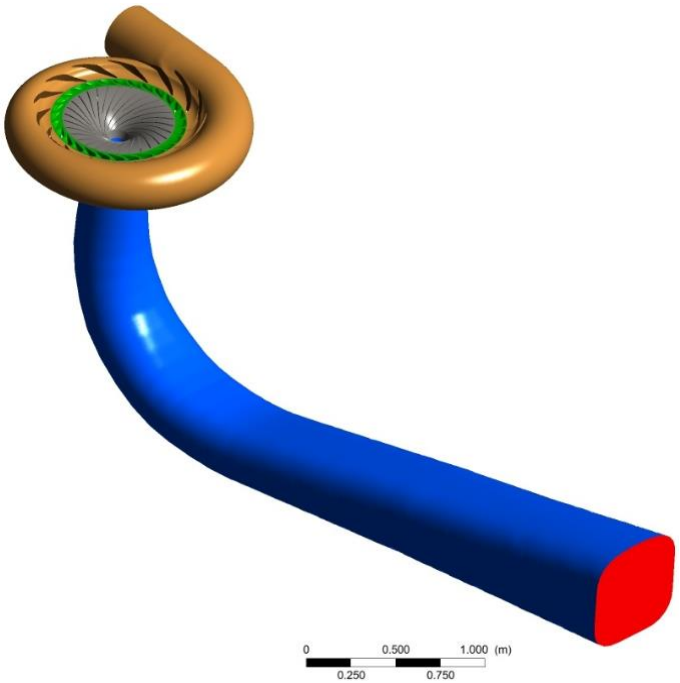

Fig.1. The computational domain.

The computations have been carried out using unstructured grids with the total number of 5,12 and to 14,28 M (million) nodes for the whole domain (Fig.2). The average distance of the

wall-nearest grid nodes normalized by the wall units, y_1^+, for the 5,12M grid was 150, for the 14,28M grid y_1^+ was 89. As seen, both grids is the coarse grid for the LES method.

To check further the grid resolution, the characteristic cell size $\Delta = (\Delta x \times \Delta y \times \Delta z)^{1/3}$ was compared with the Kolmogorov dissipative scale $L_K = \left(\nu^3 / \varepsilon\right)^{1/4}$, and the generalized Corrsin "shear" scale $L_s = \left(\varepsilon / S^3\right)^{1/2}$ (where ν is the kinematic viscosity, ε its dissipation rate (obtained from RSM), and $S = (S_{ij}S_{ij})^{1/2}$ is the strain modulus. The shear scale, characterizing the scale of the turbulence energy production, was found by Picano and Hanjalić [12] to serve well as a criterion for mesh resolution in free flows: when the grid-cell size was kept smaller than the shear scale (nominally $\Delta / L_s < 1.0$, relevant primarily in high-shear regions), the LES of a free round jet reproduced well the mean flow and turbulence statistics at very high Re number using a very coarse grid despite the cell sizes being two order of magnitude larger than the Kolmogorov scale. Fig. 3 shows the distribution of Δ/L_K *and* Δ/L_s in the central section of the turbine calculated by RSM model for part load (PL) regime for grid 5,12M.

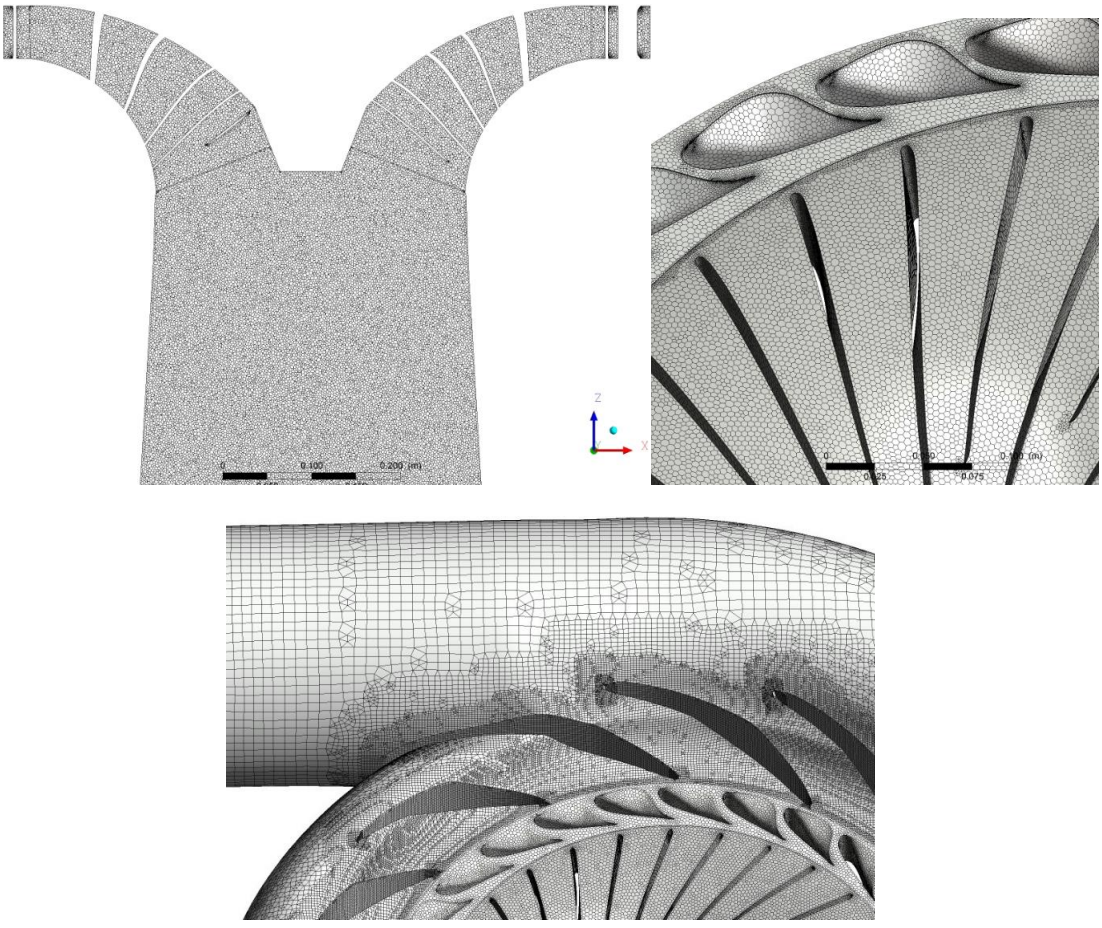

Fig.2. Views of the computational grid with 6 million nodes in the turbine model (guide vanes and runner) and its draft tube.

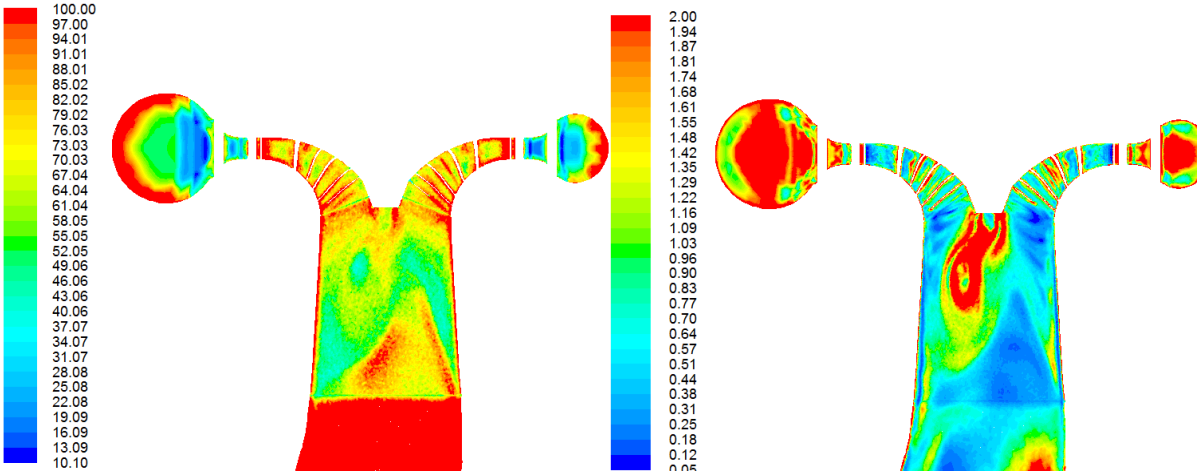

a) *b)*

Fig. 3. Grid size compared with turbulence length scales (a) Δ/L_K and (b) Δ/L_s in the middle plane turbine for 5,12M grid.

As can be seen, the ratio Δ / L_K of around 40 to 80. Interestingly, the cell-size to shear-scale ration Δ / L_S is below 1.0, except in the core region, and of course very close to the wall. This is in agreement with the findings in [12], which shows that the LES method can return satisfactory predictions when Δ / L_S is less than 1.0.

4. The results of simulations flow in the Francis-99 turbine

In this section presents the results of simulation of the flow in turbine Francis-99. Three operation point proposed for the Francis-99 (2016) workshop are calculated.

The Fig. 4 shows axial velocity in central cross-section of turbine for three operation points. Flow of HL and BEP modes are similar. Narrow concentrated vortex is formed under the runner (see Fig.5). At PL regime axial flow is close to the draft tube wall. At this operation point wide recirculation zone is formed at the axis in the draft tube cone. It is recalled that precession of the vortex core occurs under partial load (in the turbine model here considered at a discharge rate of 0.2–0.85 of the optimal value), where the flow has a considerable residual swirl. Vortex breakdown in such a flow leads to the formation of the recirculation zone at the flow axis and the rotation of the corkscrew vortex rope around it. Fig. 5 shows selected snapshots of the typical vortex ropes and their structures after the runner, captured by DES model. The ropes are identified by the instantaneous iso- surfaces of a selected values of pressure.

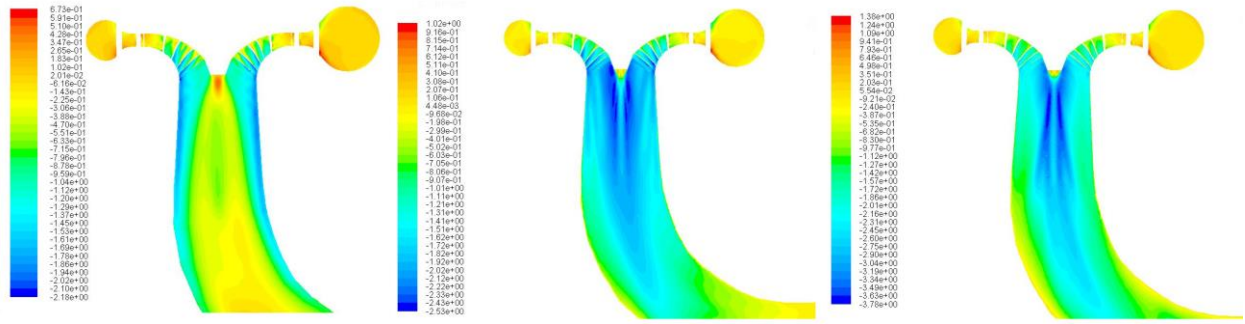

a) *b)* *c)*

Fig.4. Isolines of the axial velocity in the central section (DES model)

a) PL, b) BEP, c) HL regimes.

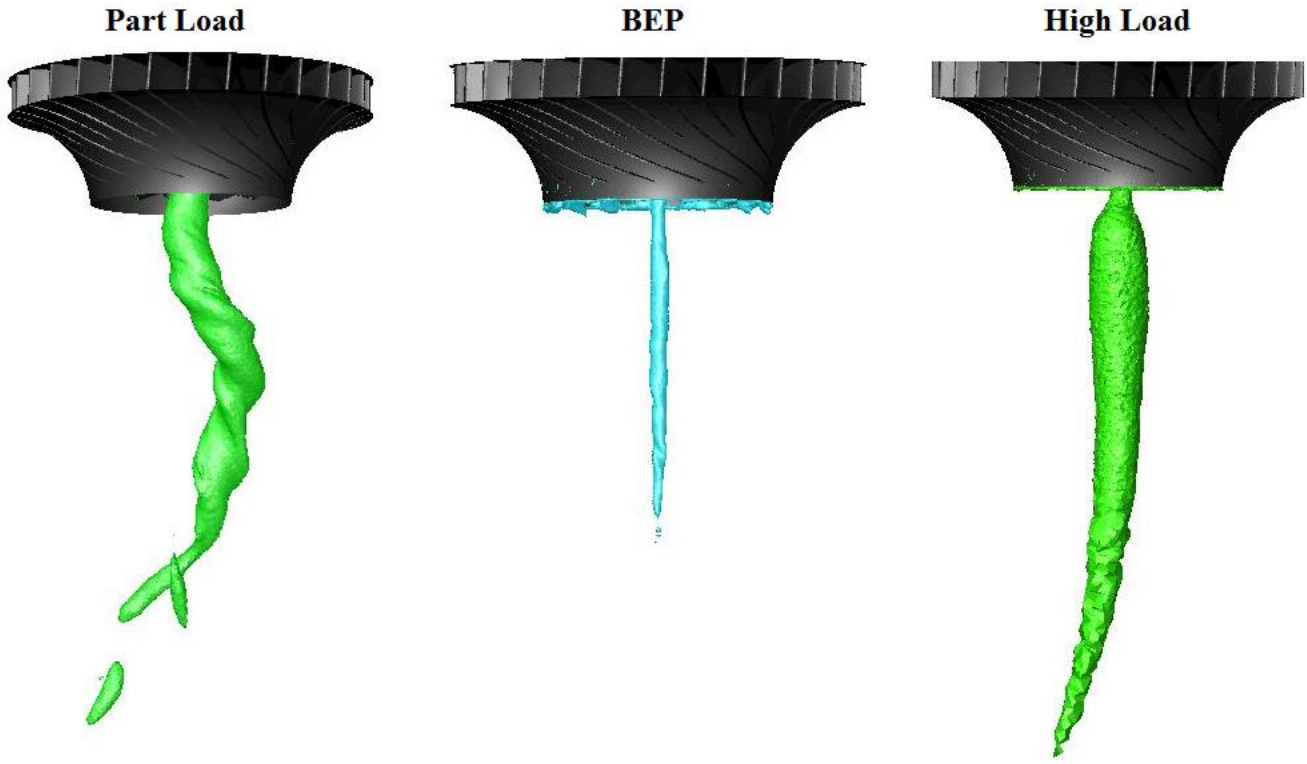

Fig.5. Vortex structure in the draft tube for different regimes (DES model)

Comparison of the calculated and experimental radial velocity profiles shown in Fig. 7,9,11. As can be seen, for all regimes of the discrepancy between calculation and experiment is very great for all turbulence models. Perhaps, this is due to the fact, that the radial velocity has lower values compared to axial and tangential velocity. Therefore, high error of measurement.

Comparison of the calculated and experimental axial velocity profiles shown in Fig. 6,8,10. As can be seen, for all regimes the calculations and experimental data agree well. The worst results for the PL regime. For this regime all computational models give the deflection of axial velocity at the center of the draft tube. The experiment has not of this trough. Use of more detailed grid does not improve the result (see Fig. 6a). The results of LES calculations for rough (5,12M) and detailed mesh (14,28M) are similar. Also it should be noted, that the difference between the different models is not very large.

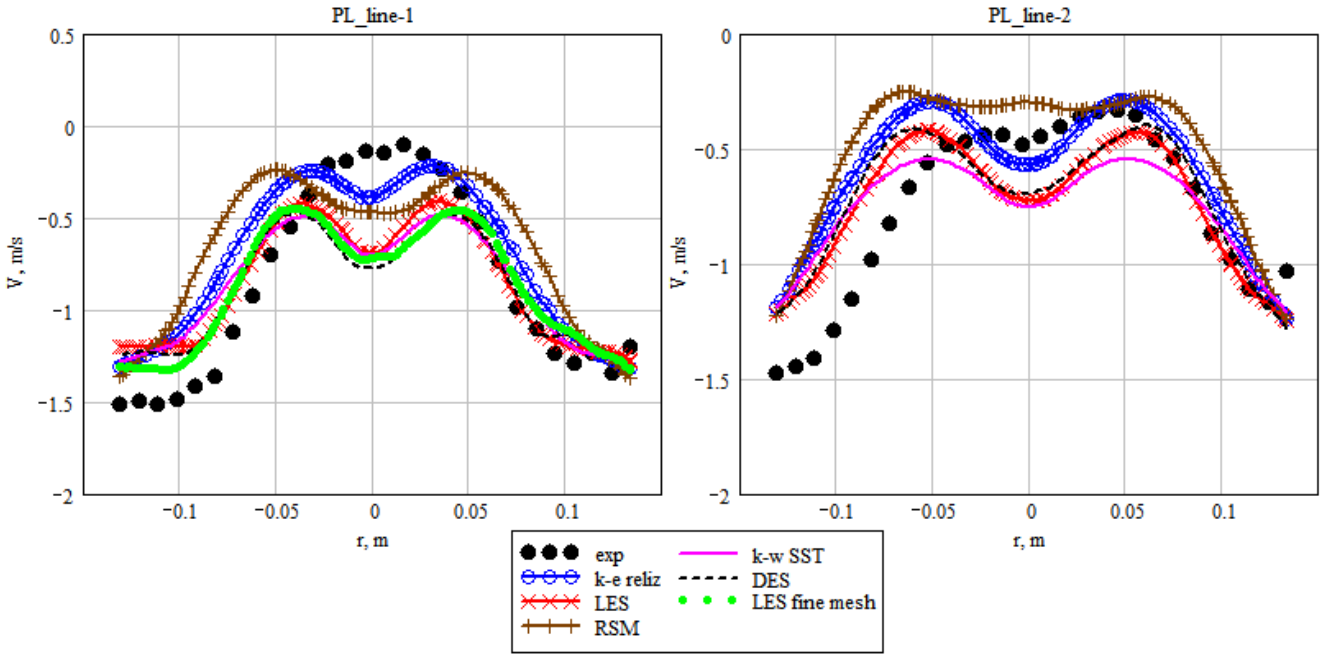

a) b)

Fig. 6. The axial component of the velocity in the line 1 (a) and line 2 (b) for PL regime.

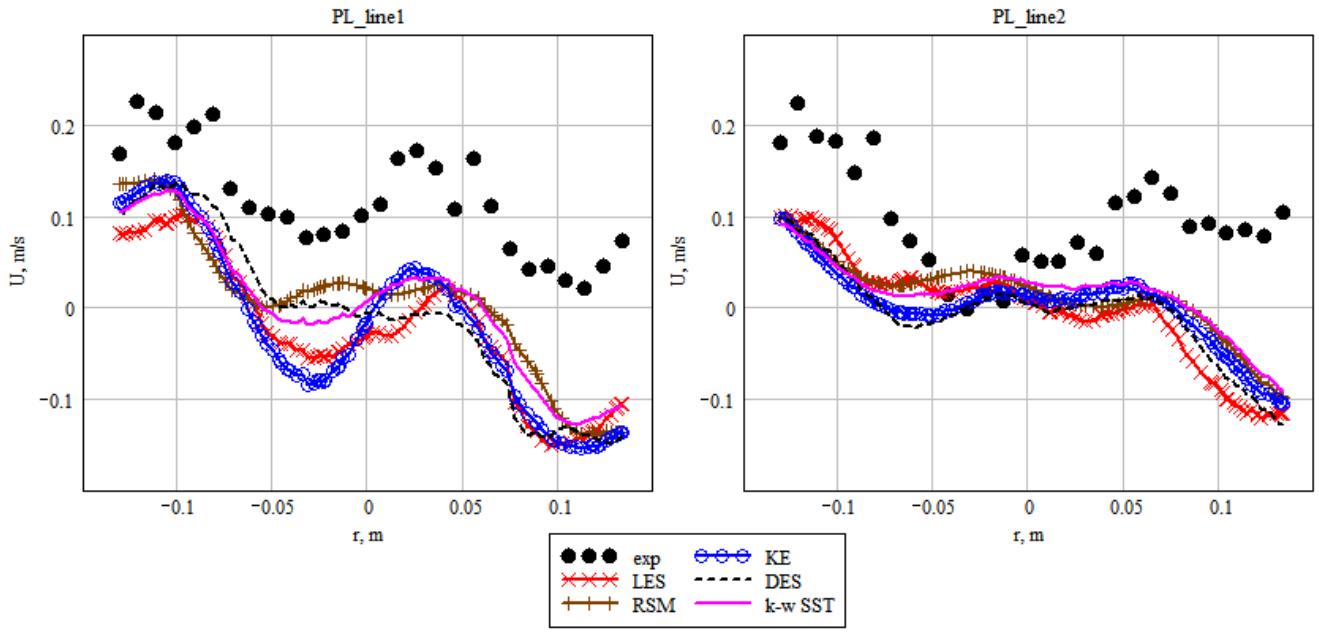

a) b)

Fig. 7. The axial component of the velocity in the line 1 (a) and line 2 (b) for PL regime.

For BEP and HL regimes the agreement between the calculation and experiment a lot better. The best agreement between the calculation and experiment is obtained for the BEP regime.

The results of the analysis of the axial velocity profiles showed that the best agreement with experiment has a LES model. The DES model also gives good results. The RANS models are close to each other. As mentioned above, the radial velocity profiles analysis does not make sense.

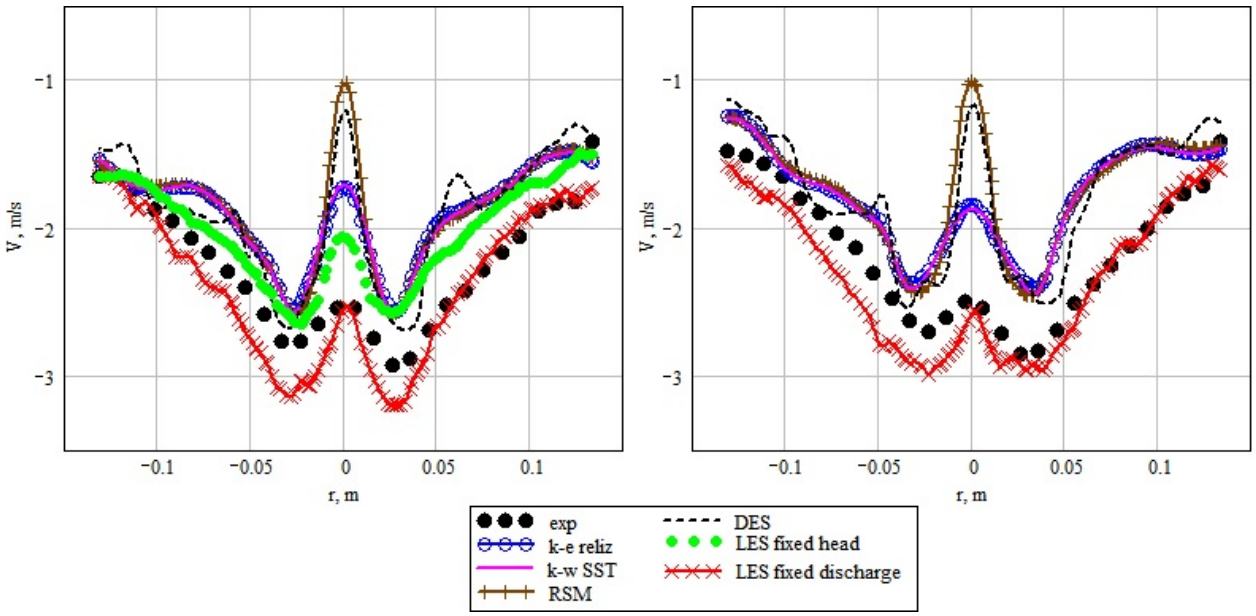

a) b)

Fig. 8. The axial component of the velocity in the line 1 (a) and line 2 (b) for BEP regime.

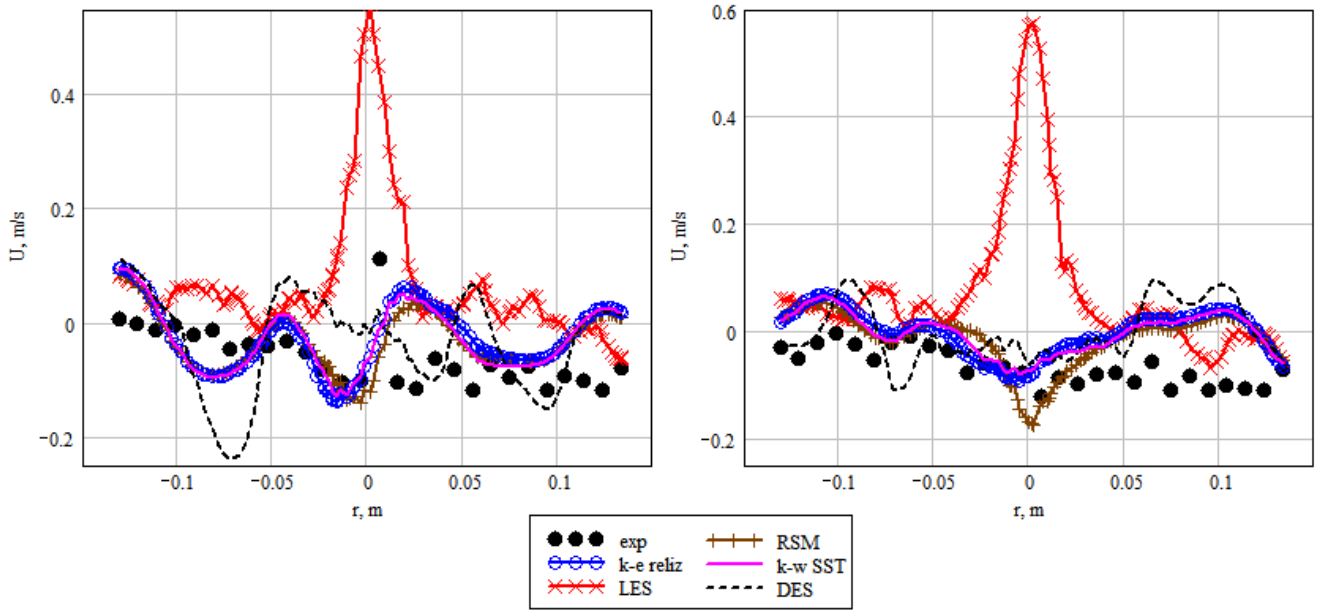

a) b)

Fig. 9. The radial component of the velocity in the line 1 (a) and line 2 (b) for BEP regime .

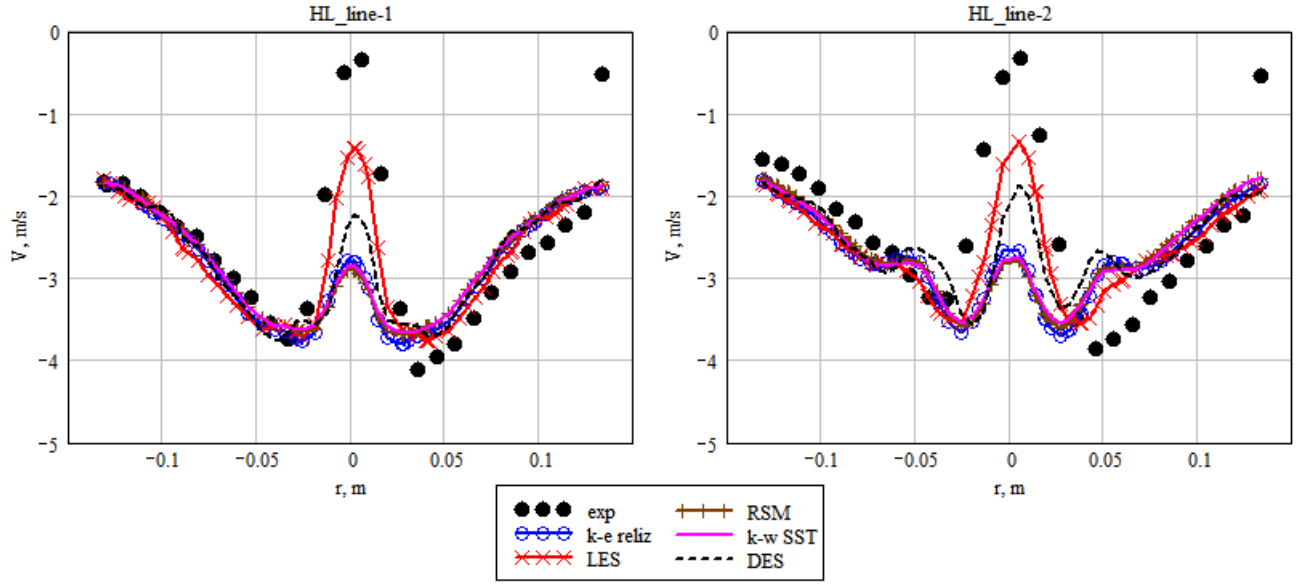

a) b)

Fig. 10. The axial component of the velocity in the line 1 (a) and line 2 (b) for HL regime.

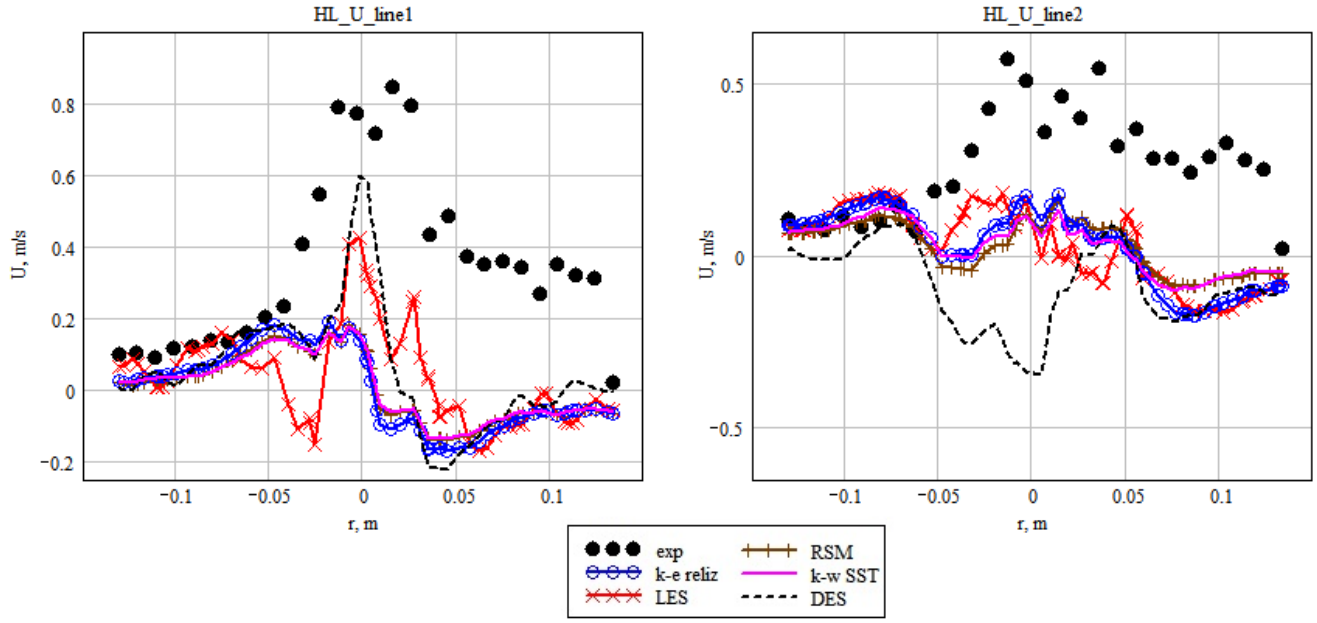

a) b)

Fig. 11. The radial component of the velocity in the line 1 (a) and line 2 (b) for HL regime.

Another reason of disagreement between calculation and experiment is a different value of discharge in the calculation and experiment. At the given a head the calculated value of discharge about 10% lower than the experimental value (see Table 2-4). For this reason, the calculated profiles are slightly higher than the experimental. If in the input of turbine set fixed value of discharge the discrepancy between experiment and simulation is significantly reduced. An example of this is shown in the Fig.8a to LES calculation.

Comparison of the calculated and experimental integral characteristics of turbine for all regimes shown in Tables 2-4. As can be seen, for all regimes calculated characteristics are 7-10% lower than the experimental value. Except of the efficiency, which calculation value the contrary overestimated in comparison with experiment. The part load operation point shows the largest discrepancy. The calculations by different turbulence models the give similar results. To say which model is best for the integral characteristics is impossible.

Table 2. Part load

Parameter	k-e reliz.	SST	RSM	DES	LES	EXP.
Net head [m]	11.87	11.87	11.87	11.87	11.87	11.87
Total torque [N m]	388.8	391.5	387.5	385.5	384.8	416.39
Discharge [kg/s]	125.46	126.95	124.6	124.32	124.5	139.6
Hydraulic efficient [%]	92.9	92.5	93.3	93.03	92.7	90.13

Table 3. Best efficiency point

Parameter	k-e reliz.	SST	RSM	DES	LES	EXP.
Net head [m]	11.94	11.94	11.94	11.94	11.94	11.94
Total torque [N m]	578.2	579.01	580.11	578.7	580.5	616.16
Discharge [kg/s]	182.8	182.9	188.59	182.2	189.2	199.6
Hydraulic efficient [%]	94.2	94.9	92.3	95.3	92.1	92.39

Table 4. High efficiency point

Parameter	k-e reliz.	SST	RSM	DES	LES	EXP.
Net head [m]	11.88	11.88	11.88	11.88	11.88	11.88
Total torque [N m]	722.8	706.8	710.4	722.86	714.2	740.54
Discharge [kg/s]	229.02	226.42	226.41	228.86	231.01	242.46
Hydraulic efficient [%]	94.6	93.6	94.1	94.7	92.74	91.71

To practice it is very important to know the level of pressure pulsation at the turbine. Therefore, it is interesting to compare the calculated and experimental values of pressure fluctuations. These data are shown in Figure 12. The plot shown of the static pressure on the draft tube wall. Pressure received at a point DT5, (see workshop web site).

For safe operation of the turbine is very important the maximum level of pressure fluctuations. Analysis of the results shows that the magnitude of pressure fluctuations experiment composes 1.68 kPa. The calculations are in good agreement with experiment (see Fig.12). So, the LES calculation give maximum of pressure fluctuations is 1.07 kPa, DES model give 0.99 kPa, and RSM model give 1.22 kPa. This is interesting, because it was previously thought that the RSM model should give the lower level of pressure fluctuations. Thus it is shown that the RSM model can be used to estimate the level of the pressure pulsations in the turbines.

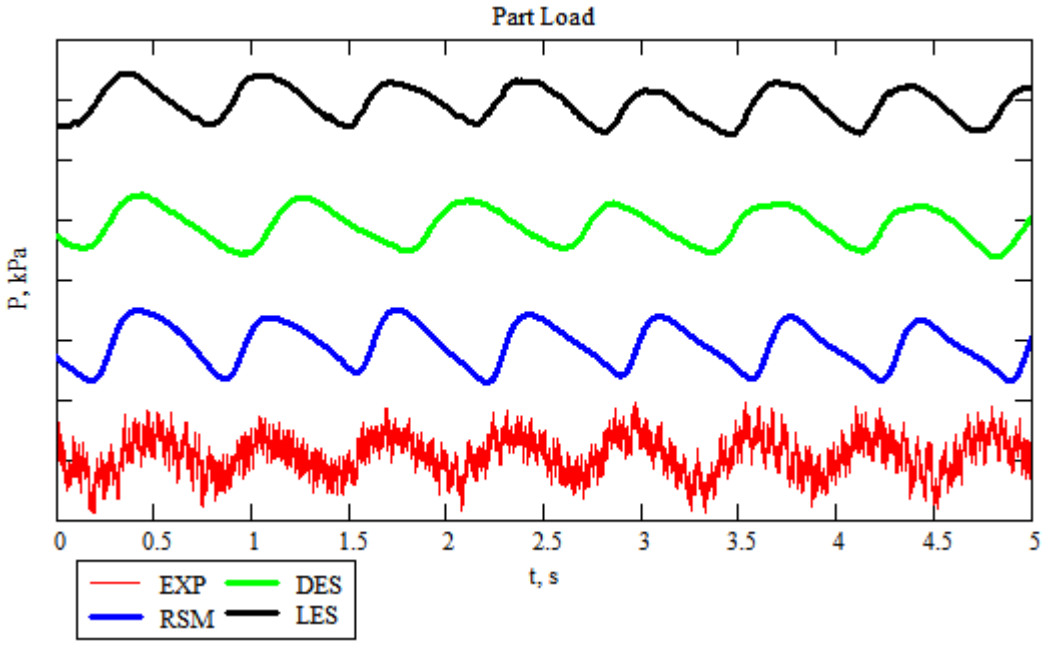

Fig. 12. The pressure pulsations at the DT5 point for Pl regime.

For analysis of pressure pulsation characteristics of the flow of great interest is the behavior of the flow structure in the turbine. Fig.13 shows a vortex structure of the flow after the runner for different unsteady models at PL regime. Flow structure is shown by the instantaneous values of iso-surfaces of pressure. We see, that in this regime is formed by vortex rope structure. In this case the LES and DES calculation gives two intertwined precessing vortex. Also is interesting that, the Reynolds stress model captures well the phenomenon, albeit with smoothed fine-scale structures. It should be noted that the URANS model also provides some transient pressure pulsation in the draft tube.

Interesting details can be observed in relation pressure pulsations and axial velocity profile downstream the turbine runner. In the modes with high pressure pulsations, the wide areas of counterflow are visible (Fig. 6). This again proves the fact that the existence of a narrow zone of counterflow on the profile of the axial velocity component may be an indicator of the intensity of transient phenomena in the turbine [4,5].

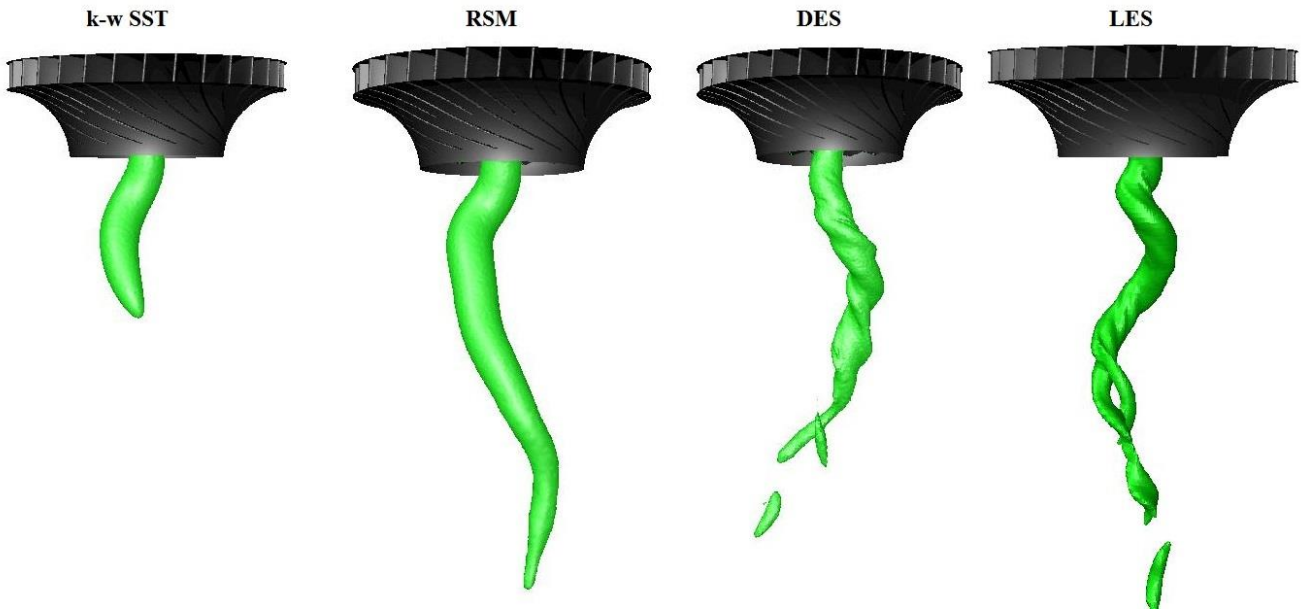

Fig.13. Vortex structure in the PL regime for different turbulence models.

In addition to the pressure pulsation it is also very important to know the frequency of pressure pulsations. It is important to estimate the potential resonance of the turbine design. A comparison by the experimental and calculated spectra is shown in Figure 14 pressure. The flow after the runner have precessing vortex structures (Fig. 13). For this reason, spectrum have one dominant frequency. In the experiment frequency of pressure pulsations for this regime is 1,53Hz. This frequency is the frequency of precession of intense main vortex core.

As it is obvious from the spectrum of pressure pulsations, the calculation results are well proved by the experiment, both for the frequency and intensity of pulsations. The LES calculation it provides frequency 1,57 Hz, DES it provides frequency 1,22 Hz. And the RSM calculation it provides frequency 1,47 Hz.

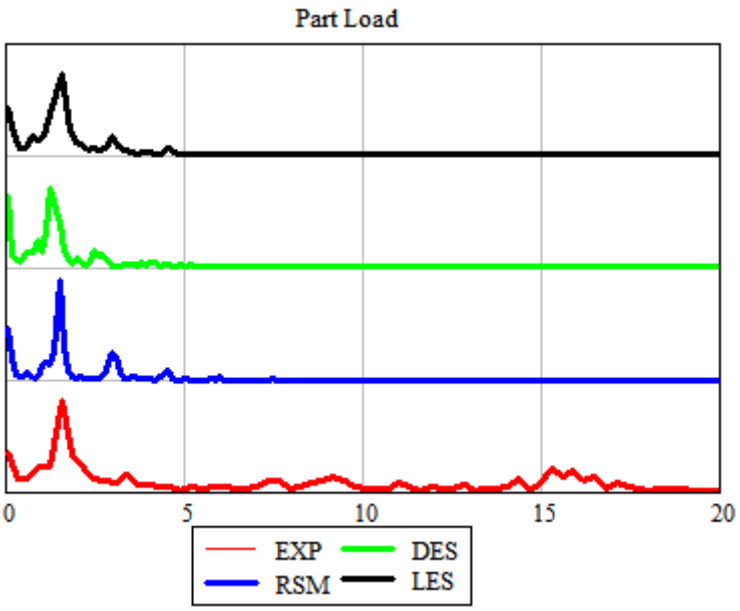

Fig. 14. The spectrum of pressure pulsations at the DT5 point for Pl regime.

5. Conclusions

The paper presents the results of numerical simulation of flow in a laboratory model of a Francis hydroturbine at a three regimes, using two eddy-viscosity- (EVM) and a Reynolds stress (RSM) RANS models (realizable k-ε, k-ω SST, LRR) and detached-eddy-simulations (DES), as well as large-eddy simulations (LES). Three operation point proposed for the Francis-99 workshop are calculated. Comparison of calculation results with the experimental data was carried out.

The results of the analysis of the axial velocity profiles showed that the best agreement with experiment has a LES model. The DES model also gives good results. The RANS models are close to each other.

The worst results for the PL regime. For BEP and HL regimes the agreement between the calculation and experiment a lot better. The best agreement between the calculation and experiment is obtained for the BEP regime.

The structure of the flow behind the runner was analyzed by numerical simulation, which revealed the effect of the flow structures on the frequency and intensity of the pulsations. The calculations confirmed that a vortex rope behind the runner is the main cause of low-frequency pressure pulsations in hydraulic turbines. Its dynamics determines predominantly the behavior of turbine pulsations.

Acknowledgement

This work was supported in part by the Russian Foundation for Basic Research.

REFERENCES

1. Nicolet C. Hydroacoustic modelling and numerical simulation of unsteady operation of hydroelectric systems PhD Thesis (EPFL № 3751, http://library.epfl.ch/theses/?nr=3751), 2007.

2. Doerfler P. System dynamics of the Francis turbine half load surge. IAHR Symp. on Hydraulic Machinery and Systems, Amsterdam, Netherlands, 1982.

3. Ruprecht, A. Numerical prediction of vortex instabilities in turbomachinery // Notes on Numerical Fluid Mechanics and Multidisciplinary Design, Springer Verlag. 2006. Vol. 93, p.211-224.

4. Minakov A.V., Platonov D.V., Dekterev A.A., Sentyabov A.V., Zakharov A.V. The analysis of unsteady flow structure and low frequency pressure pulsations in the high-head Francis turbines // International Journal of Heat and Fluid Flow, 2015, Vol. 53, pp. 183 – 194

5. Minakov A.V., Platonov D.V., Dekterev A.A., Sentyabov A.V., Zakharov A.V. The numerical simulation of low frequency pressure pulsations in the high-head Francis turbine // Computers and Fluids, Vol. 111, April 2015, pp. 197 – 205. doi:10.1016/j.compfluid.2015.01.007

6. Alligne S., Maruzewski P., Dinh T., Wang B., Fedorov A., Iosfin J. and Avellan F., 2010, Prediction of a Francis turbine prototype full load instability from investigations on the reduced scale model. Proc. IAHR Symp. on Hydraulic Machinery and Systems, Timisoara, Romania.

7. Cervantes M.J., Engstrom T.F., Gustavsson L.H., 2005, Proc. The third IAHR/ERCOFTAC workshop on draft tube flows Turbine 99. Sweden, Porjus,. 193 p.

8. Minakov, A.V. Sentyabov, D.V. Platonov, A.A. Dekterev, A.A. Gavrilov, 2014, Numerical modeling of flow in the Francis-99 turbine with Reynolds stress model and detached eddy simulation method. Journal of Physics: Conference Series Volume 579, doi:10.1088/1742-6596/579/1/012004.

9. Gavrilov A., Dekterev A., Sentyabov A., Minakov A., Platonov D. Application of hybrid methods to calculations of vortex precession in swirling flows // Notes on Numerical Fluid Mechanics. 2012. vol. 117. P. 449-459.

10. Kuznetsov I., Zakharov, A., Orekhov, G., Minakov, A., Dekterev, A., Platonov, D. Investigation of free discharge through the hydro units of high head Francis turbine. IOP Conference Series: Earth and Environmental Science 15 (PART 5). 2012. doi: 10.1088/1755-1315/15/5/052002

11. Smirnov, R., Shi, S., Celik, I., 2001, Random flow generation technique for large-eddy simulations and particle-dynamics modeling, *J. Fluids Engineering*. 123: 359–371.

12. Picano, S. and Hanjalić, K., 2012, Leray-α regularization of the Smagorinsky-closed filtered equations for turbulent jets at high Reynolds numbers, Flow, Turbulence and Combustion, 89: 627–650.